Computational Sciences and Engineering

journal homepage: https://cse.guilan.ac.ir/

University of Guilan

Application of Skyhook Control Strategy to Semi-active Suspension System with Magneto-Rheological (M.R) Damper for Improving the Performance of Vehicle Suspension System Traversing Steady State Road Conditions

Arinola Bola Ajayi [a,*], Sunday Joshua Ojolo [a], Ediketin Ojogho [b]

[a] Dept of Mech. Engr. University of Lagos, Lagos, Nigeria
[b] Dept. of Aerospace Engr. Lagos State University, Epe Campus, Lagos State, Nigeria

A B S T R A C T

In this paper, skyhook control strategy was applied to semi-active suspension system with magneto-rheological (M.R) damper to improve the performance of the suspension system of a vehicle traveling on a road with steady state conditions. When a vehicle travels over uneven roads at different speeds, the sprung mass and unsprung mass undertake various movements that make the chassis and driving to respond dynamically, which may affect severely the rider's comfort and general health. In order to reduce the health hazards posed by uneven roads, skyhook control strategy was applied to vehicle suspension system. The effect of the skyhook control strategy on the suspension system of the vehicle was modeled and investigated by using MATLAB/Simulink software. The outcome was compared with suspension systems without a skyhook control strategy. The results show that the weighted rms vertical acceleration value of the vehicle body reduced thereby leading to the reduction in the discomfort experienced by the riders due to the implementation of skyhook control strategy.

1. Introduction

Riders in vehicles traveling over uneven roads usually feel uncomfortable notwithstanding that the vehicle's suspension system is designed to separate the body of the vehicle and its occupants from the vertical accelerations and vibrations created by the uneven road. When a vehicle travels over uneven terrain at varying speeds, its sprung mass and unsprung mass move in divers' ways, which affects the chassis' dynamic response, driving dynamics, vehicle's brake dynamics, convenience of the passengers, safety, and the stability of the vehicle [1]. Responses of riders on a vehicle traveling on an uneven road were assessed by using standard comfort parameters. The rider's

---

response to vibrating frequency, the excitation variations and the extent of exposure all significant factors in how comfortable a vehicle's ride is [2]. In a study experiment in which 30 men and 30

women were seated freely on a vibrating plate and were exposed to vibrating input for 8 second, their responses were assessed [3]. An experiment was carried out with 16 participants, using six automotive seats with different combinations attached to a vibrator [4]. In another experiment, the level of vibration of the seat was taking into consideration in quantifying the discomfort of the dynamic effects of the vehicle [5]. A model of half-car semi-active suspension system was used in conjunction with human-seat arrangement by another experimenter. The suspension characteristics of the vehicle as well as the human biomechanical parameters were used in a study to evaluate the discomfort felt by vehicle passengers traveling on an uneven road. The excitation input into the vehicle suspension system was a half sine bump on a smooth road for the vehicle to pass over it as transient road condition. Vibration dosage value (VDV) was used to assess the degree of discomfort felt by the riders while the vehicle transverses the uneven road [6]. The vibrating input of a semi-active vehicle suspension system traveling on a steady-state road conditions such as smooth, gravel, and suburban roads was examined for the purpose of deriving mathematical equations based on the consideration of the vehicle's pitch and heave motions. Power spectral density, PSD, was used to classify the input spectrum of the road characteristics based on road roughness characteristics that agree with the International Roughness Index (IRI). The discomfort experienced by the riders on the gravel and suburban roads were observed to have increased as the vehicle's input parameters were increased. It was concluded that in order to obtain a comfortable ride that is within the human comfort zone for the gravel and suburban roads conditions, the speed vehicle should be reduced below 20 km/h or there should be an appropriate modification of the suspension systems [7].

Researchers have utilized several control methods to increase car suspension system performance and minimize human rider discomfort on vehicles. Suspension system control is the capability of the suspension system to offer stability with a high level of ride comfort, safety, and handling, while reducing passengers' discomfort during vehicle travel over uneven road surfaces. As a result, the control procedure entails determining the best design variables for stiffness and damping coefficients to reduce the sprung mass acceleration and the displacement of the suspension [8]. Due to the challenges or setbacks in the use of servo-driven dry friction design in active suspension system, algorithm to identify control and diagnose suspension system faults was developed [9]. Servo-driven dry friction damper was used in a suspension system of a car to improve vehicle performance as a substitute to regular viscous damper [10]. Sliding mode controller was used to improve vibration control performance of a semi-active electro-rheological seat suspension system while an adaptive sliding mode controller with fuzzy compensation with H infinity was used to control a quarter car active suspension system [11 – 12].

The suspension systems that are semi-active can vary the parameters of the suspension systems in line with the control strategy to achieve an outcome that is satisfying on different road conditions [13 – 15]. Semi-active suspension system is made up of dampers that are controllable with passive springs that requiring little energy source in other not to destabilized the control [16 – 17]. Semi-active dampers of various configurations have been investigated in the past. The most common among them are magneto-rheological dampers, M.R whose response varies with magnetic field applied and electro-rheological damper with its response varying with the applied electric field [18]. The commonly utilized improvement for semi-active suspension system is the skyhook

control strategy. It for mitigating the vehicle body vibration independent of the vibration source and doubles as optimal control method used for minimizing the root-mean-square, rms, value of the sprung mass acceleration of vehicle suspension system to obtain optimum ride comfort. The skyhook gain, is a damping parameter of a fictitious damper. The skyhook control is not difficult to implement, only a few information about the state of the vehicle is required. It imagines a virtual damper in between the vehicle body (sprung mass) and an imaginary sky [19]. Although, it is effective in enhancing the characteristics ride comfort of vehicle but the dynamic tire force is impacted negatively at the same time. The variable quantities are the velocity of the sprung mass, and the relative velocity between the sprung mass and unsprung mass. When the velocity of the vehicle body relative to the wheel (unsprung mass) is in the same direction with the velocity of the sprung mass, this will result in a maximum damping force being applied to reduce the acceleration of the body. On the contrary, when the two velocities are in the opposite directions, the body acceleration will be reduced due to minimum damping force [20]. The resonant peak of the vehicle body mass response will be reduced due to skyhook control to be able to obtain a ride quality that is good. Also, the use of high damping force as a control measure for semi-active suspension system were also utilized in the past [20 – 21]. Skyhook control strategy improves ride comfort as well as improves vehicle handling by stabilizing the vehicle body motion [8]. Instead of computing the intended damper force by direct variable optimization, another technique by computing the force so that the real system approximates the behavior of the ideal system [19]. The skyhook controller controls vehicle system by acting like an invincible damper attached to one of the ends of the sprung mass while the other end is fixed to an arbitrary point in the skyhook [15]. Magneto-rheological dampers, MR, which act as actuators are positioned between the sprung mass and the unsprung mass to activates the skyhook damper force without any external power source [8]. The objective of the study is to apply skyhook control strategy with MR damper in vibration control to half-car model to improve the performance of suspension system of vehicle when traveling on steady state road conditions. The half-car and human-seat 7 degree of freedom model used gives better approximations to real life situations than quarter-car models used in the past.

2. Methodology

2.1 Mathematical Modeling

The study is to be carried out using a 7-degree of freedom model, shown in Figure 1, which is made up of a 4-degree of freedom half-car suspension model, and a 3-degree of freedom human-seat arrangement. The human system is assumed as a biomechanical system with stiffness and damping properties. The point C in the diagram is the driver/passenger position while the distance between the body of the vehicle and the seat-driver subsystem is Point B and it is located some distance from the vehicle body center of gravity.

In this model, two skyhook control dampers are connected to the vehicle body at the front and at the rear. The unsprung mass vibration remains without damping force with this configuration, that is the dampers in the unsprung mass disappears. In this study, magneto-rheological dampers, MR are used as actuators or control dampers. The skyhook damper forces are stimulated by the dampers without applying power source externally, but just by suspension energy being dissipated. The reduction of the sprung mass excitation is attained from the unsprung mass'

vibration. As a result, there is a high wheel bouncing, leading to poor contact between the tire and the road surface. The ideal skyhook control strategy is purposeful if priority is given to the control of the vibration of the sprung mass or the ride comfort of the vehicle.
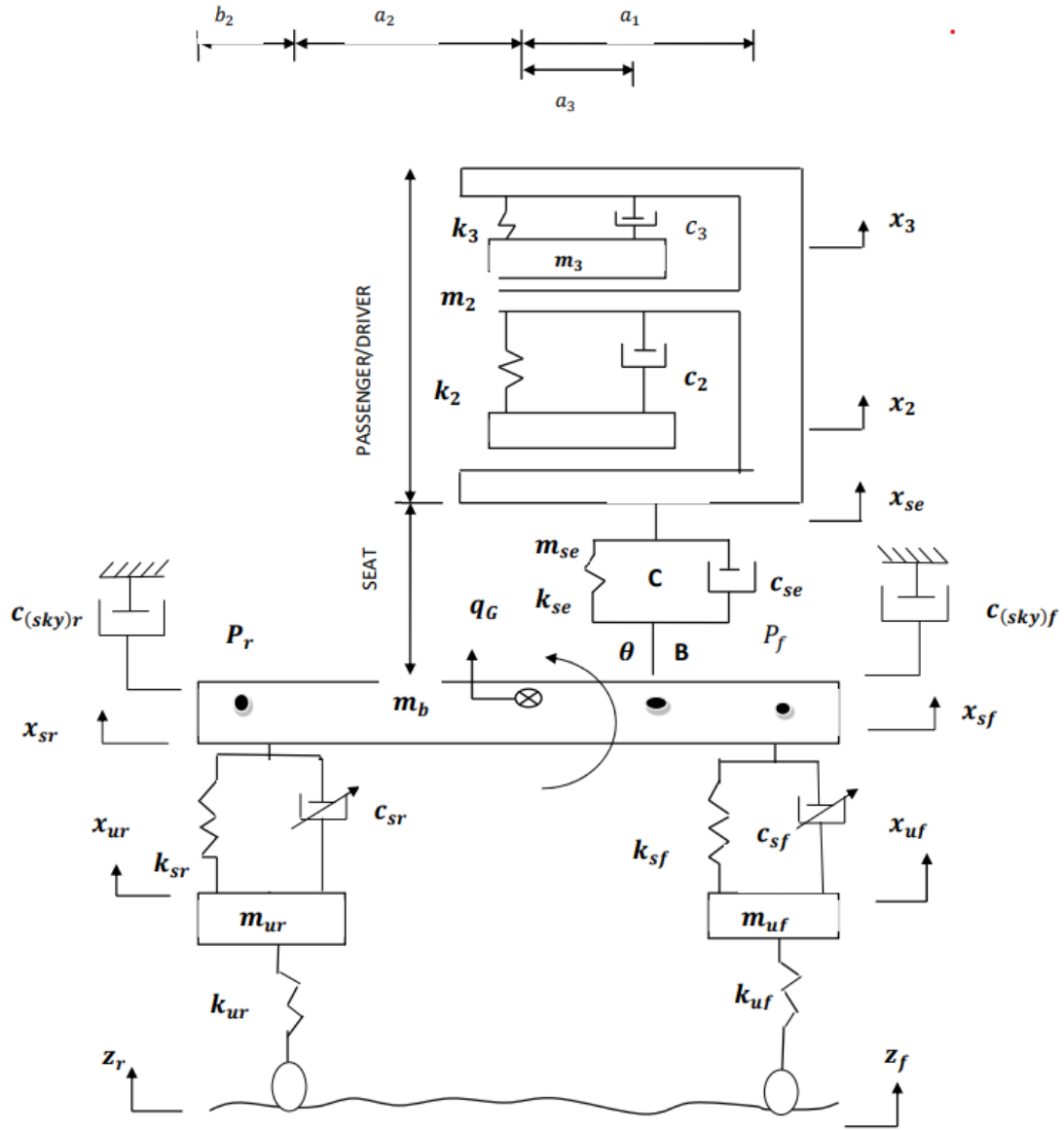
Figure. 1: Skyhook control for semi-active suspension system.

The force generated by skyhook at the front suspension given in **Eq. (1)** as:

$$F_{(sh)f} = c_{(sh)f} \dot{x}_{sf} \tag{1}$$

The force generated by the MR damper at front suspension is given as **Eq. (2)**

$$F_{(d)f} = c_{(sh)f} \left(\dot{x}_{sf} - \dot{x}_{uf} \right) \tag{2}$$

The forces must be equal. This gives **Eq. 3**,

$$c_{sf} \left(\dot{x}_{sf} - \dot{x}_{uf} \right) = c_{(sh)f} \dot{x}_{sf} \tag{3}$$

Similarly,

The force generated by the MR damper on the rear suspension is equal to the force on the rear skyhook damper and it is given **Eq. (4)**

$$c_{sr}(\dot{x}_{sr} - \dot{x}_{ur}) = c_{(sh)r}\dot{x}_{sr} \tag{4}$$

However, the damper generating the damping force is always in the reverse direction of the suspension movement. Thus, the conditions applicable for the front and rear skyhook are given in **Eq. 5** and **Eq. 6** respectively:

For the front skyhook control

$$F_{(sh)f} = \begin{cases} c_{sf}(\dot{x}_{sf} - \dot{x}_{uf}) & if \;\; x_{sf}(\dot{x}_{sf} - \dot{x}_{uf}) \geq 0 \\ 0 & if \;\; x_{sf}(\dot{x}_{sf} - \dot{x}_{uf}) < 0 \end{cases} \tag{5}$$

For the rear skyhook control

$$F_{(sh)r} = \begin{cases} c_{sr}(\dot{x}_{sr} - \dot{x}_{ur}) & if \;\; x_{sr}(\dot{x}_{sr} - \dot{x}_{ur}) \geq 0 \\ 0 & if \;\; x_{sr}(\dot{x}_{sr} - \dot{x}_{ur}) < 0 \end{cases} \tag{6}$$

The 7-degree of freedom resulting from half-car and human-seat suspension models using the skyhook control strategy are governed by **Eq. 7(a, b)** and **Eq. 8(a, b)**.

$$m_3\ddot{x}_3 + c_3(\dot{x}_3 - \dot{x}_{se}) + k_3(x_3 - x_{se}) = 0 \tag{7a}$$

$$m_3\ddot{x}_3 + c_3\dot{x}_3 - c_3\dot{x}_{xe} + k_3x_3 - k_3x_{se} = 0 \tag{7b}$$

$$m_2\ddot{x}_2 + c_2(\dot{x}_2 - \dot{x}_{se}) + k_2(x_2 - x_{se}) = 0 \tag{8a}$$

$$m_2\ddot{x}_2 + c_2\dot{x}_2 - c_2\dot{x}_{se} + k_2x_2 - k_2x_{se} = 0 \tag{8b}$$

When there is small rotation by the seat about the center of gravity of the sprung mass at a distance a_3, the approximation of the vertical displacement of the seat is **Eq. (9)**

$$q_b = x_b - a_3\theta \tag{9}$$

The first-time derivative of **Eq. (9)** is **Eq. (10)**

$$\dot{q}_b = \dot{x}_b - a_3\dot{\theta} \tag{10}$$

The dynamic equation of the seat is given in **Eq. (11)**

$$m_{se}\ddot{x}_{se} + c_{se}\dot{x}_{se} - c_{se}(\dot{x}_b - a_3\dot{\theta}) + c_2(\dot{x}_{se} - \dot{x}_2) + c_3(\dot{x}_{se} - \dot{x}_3) + k_{se}x_{se} \\ - k_{se}(x_b - a_3\theta) + k_2(x_{se} - x_2) + k_3(x_{se} - x_3) = 0 \tag{11}$$

In **Eq. 11,** simplifying and collating the like terms gives **Eq. 12**

$$m_{se}\ddot{x}_{se} + (c_{se} + c_2 + c_3)\dot{x}_{se} + c_{se}a_3\dot{\theta} - c_{se}\dot{x}_b - c_2\dot{x}_2 - c_3\dot{x}_3 + (k_{se} + k_2 + k_3)x_{se} - k_{se}x_b \\ + k_{se}a_3\theta - k_2x_2 - k_3x_3 = 0 \tag{12}$$

By using the skyhook control strategy, the differential equations describing the motion of the semi-active half-car suspension system for the sprung mass motion is given in **Eq. (13)** as,

$$m_b\ddot{x}_b + c_{sf}(\dot{x}_{sf} - \dot{x}_{uf}) + k_{sf}(x_{sf} - x_{uf}) + c_{sr}(\dot{x}_{sr} - \dot{x}_{ur}) + k_{sr}(x_{sr} - x_{ur}) + c_{se}\dot{q}_b - k_{se}q_b$$
$$+ c_{se}\dot{x}_{se} + k_{se}x_{se} = 0 \tag{13}$$

Substituting **Eq. (3)** and **Eq. (4)** into **Eq. (13)**, will give **Eq. (14)**

$$m_b\ddot{x}_b + c_{(sh)f}\dot{x}_{sf} + k_{sf}(x_{sf} - x_{uf}) + c_{(sh)r}\dot{x}_{sr} + k_{sr}(x_{sr} - x_{ur}) + k_{sr}(x_{sr} - x_{ur}) + c_{se}\dot{q}_b - k_{se}q_b$$
$$+ c_{se}\dot{x}_{se} + k_{se}x_{se} = 0 \tag{14}$$

Assuming the body of the vehicle undergoes small rotation about its center of gravity CG, the vertical displacements of the front sprung mass and the rear sprung mass are **Eq. (15)** and **Eq. (16)** respectively

$$x_{sf} = x_b - a_1\theta \tag{15}$$

$$x_{sr} = x_b + a_2\theta \tag{16}$$

The first time derivates of the front sprung mass and the rear sprung mass are given in **Eq. (17)** and **Eq. (18)** respectively.

$$\dot{x}_{sf} = \dot{x}_b - a_1\dot{\theta} \tag{17}$$

$$\dot{x}_{sr} = \dot{x}_b + a_2\dot{\theta} \tag{18}$$

Substituting **Eq. (9)**, **Eq. (10)** and **Eq. (15 – 18)** into **Eq. (14)** gives **Eq. (19)**

$$m_b\ddot{x}_b + c_{(sh)f}(x_b - a_1\theta) + k_{sf}(x_b - a_1\theta - x_{uf}) + c_{(sh)r}(x_b + a_2\theta)$$
$$+ k_{sr}(x_b + a_2\theta - x_{ur}) + c_{se}(\dot{x}_b - a_3\dot{\theta}) + k_{se}(x_b - a_3\theta) - c_{se}\dot{x}_{se}$$
$$+ k_{se}x_{se} = 0 \tag{19}$$

Re-arranging **Eq. (19)** gives **Eq. (20)**

$$m_b\ddot{x}_b + (c_{(sh)f} + c_{(sh)r} + c_{se})\dot{x}_b + (c_{(sh)r}a_2 - c_{(sh)f}a_1 - a_3c_{se})\dot{\theta}$$
$$+ (k_{sf} + k_{sr} + k_{se})x_b + (k_{sr}a_2 - k_{sf}a_1 - a_3k_{se})\theta - k_{sf}x_{uf}$$
$$- k_{sr}x_{ur} - c_{se}\dot{x}_{se} - k_{se}x_{se} = 0 \tag{20}$$

The dynamic equation for the unsprung mass (frontal section) is given in **Eqn. 21**:

$$m_{uf}\ddot{x}_{uf} + c_{sf}(\dot{x}_{uf} - \dot{x}_{sf}) + k_{sf}(x_{uf} - x_{sf}) + k_{uf}(x_{uf} - z_f) = 0 \tag{21}$$

Re-arranging **Eq. (21)** gives **Eq. (22)**

$$m_{uf}\ddot{x}_{uf} + c_{sf}\dot{x}_{sf} + k_{sf}(x_{uf} - x_{sf}) + k_{uf}(x_{uf} - z_f) = 0 \tag{22}$$

Substituting **Eq. (3)** and **Eq. (18)** into **Eq. (22)** which gives **Eq. (23)**, the dynamic equation with Skyhook effect

$$m_{uf}\ddot{x}_{uf} - c_{(sh)f}(\dot{x}_b - a_1\dot{\theta}) + k_{xf}(x_{uf} - x_b + a_1\theta) + k_{uf}(x_{uf} - z_f) = 0 \tag{23}$$

Simplifying and re-arranging **Eq. (23)** will give **Eq. (24)**

$$m_{uf}\ddot{x}_{uf} - c_{(sh)f}\dot{x}_b + c_{(sh)f}a_1\dot{\theta} + (k_{sf} + k_{uf})x_{uf} - k_{sf}x_b + k_{sf}a_1\theta - k_{uf}z_f = 0 \tag{24}$$

Eq. (25) is dynamic equation of the unsprung mass (rear)

$$m_{ur}\ddot{x}_{ur} + c_{sr}(\dot{x}_{ur} - \dot{x}_{sr}) + k_{sr}(x_{ur} - x_{sr}) + k_{ur}(x_{ur} - z_r) = 0 \tag{25}$$

Substituting **Eq. (4)** into **Eq. (25)** and re-arranging gives **Eq. (26)**

$$m_{ur}\ddot{x}_{ur} - c_{(sh)r}\dot{x}_{sr} + k_{sr}(x_{ur} - x_{sr}) + k_{ur}(x_{ur} - z_r) = 0 \tag{26}$$

Substituting **Eq. (18)** into **Eq. (26)** gives **Eq. (27)** thus,

$$m_{ur}\ddot{x}_{ur} - c_{(sh)r}(\dot{x}_b + a_2\dot{\theta}) + k_{sr}(x_{ur} - x_b - a_2\theta) + k_{ur}(x_{ur} - z_r) = 0 \tag{271}$$

Rearranging **Eq. (27)** gives **Eq. (28)**

$$m_{ur}\ddot{x}_{ur} - c_{(sh)r}\dot{x}_b - c_{(sh)r}a_2\dot{\theta} + (k_{sr} + k_{ur})x_{ur} - k_{sr}x_b - k_{sr}a_2\theta - k_{ur}z_r = 0 \tag{28}$$

For the pitch motion of the sprung mass; the dynamic equation of the sprung mass rotation about its lateral axis is given in **Eq. (29).**

$$\begin{aligned} J\ddot{\theta} - a_1 c_{sf}(\dot{x}_{sf} - \dot{x}_{uf}) + a_1 k_{sf}(x_{sf} - x_{uf}) + a_2 c_{sr}(\dot{x}_{sr} - \dot{x}_{ur}) \\ + a_2 k_{sr}(x_{sr} - x_{ur}) + a_3 c_{se}\dot{q}_b + a_3 k_{se}q_b - a_3 k_{se}x_{se} - a_3 c_{se}\dot{x}_{se} = 0 \end{aligned} \tag{29}$$

Substituting **Eq. (3)** and **Eq. (4)** into **Eq. (29)** gives **Eq. (30)**

$$\begin{aligned} J\ddot{\theta} - a_1 c_{(sh)f}\dot{x}_{sf} + a_1 k_{sf}(x_{sf} - x_{uf}) + a_2 c_{(sh)r}\dot{x}_{sr} + a_2 k_{sr}(x_{sr} - x_{ur}) + a_3 c_{se}\dot{q}_b + a_3 k_{se}q_b \\ - a_3 k_{se}x_{se} - a_3 c_{se}\dot{x}_{se} = 0 \end{aligned} \tag{30}$$

Substituting **Eq. (9), (10), (15), (16), (17),** and **(18)**, into **Eq. (30)** gives **Eq. (31)**

$$\begin{aligned} J\ddot{\theta} - a_1 c_{(sh)f}(\dot{x}_b - a_1\dot{\theta}) - a_1 k_{sf}(x_b - a_1\theta - x_{uf}) + a_2 c_{(sh)r}(\dot{x}_b + a_2\dot{\theta}) + a_2 k_{sr}(x_b + a_2\theta - x_{ur}) \\ + a_3 c_{se}(\dot{x}_b - a_3\dot{\theta}) + a_3 k_{se}(x_b - a_3\theta) - a_3 k_{se}x_{se} - a_3 c_{se}\dot{x}_{se} = 0 \end{aligned} \tag{31}$$

Simplifying **Eq. (31)** gives **Eq. (32)**

$$\begin{aligned} J\ddot{\theta} + (a_2 c_{(sh)r} - a_1 c_{(sh)f} + a_3 c_{se})\dot{x}_b + (a_2{}^2 c_{(sh)r} + a_1{}^2 c_{(sh)f} + a_3{}^2 c_{se})\dot{\theta} \\ + (a_2 k_{sr} - a_1 k_{sf} + a_3 k_{se})x_b + (a_1{}^2 k_{sf} + a_2{}^2 k_{sr} + a_3{}^2 k_{se})\theta + a_1 k_{sf}x_{uf} \\ - a_2 k_{sr}x_{ur} - a_3 k_{se}x_{se} - a_3 c_{se}\dot{x}_{se} = 0 \end{aligned} \tag{32}$$

Combining **Eq. (7b), (8b), (12), (20), (24), (28)** and **Eq. (32)** to form **Eq. (33)** in matrix form, thus describing the generalized system equations of motion:

$$[M]\{\ddot{x}\} + [C]\{\dot{x}\} + [K]\{x\} = \{F\} \tag{33}$$

$$[M] = \begin{bmatrix} m_3 & 0 & 0 & 0 & 0 & 0 & 0 \\ 0 & m_2 & 0 & 0 & 0 & 0 & 0 \\ 0 & 0 & m_{se} & 0 & 0 & 0 & 0 \\ 0 & 0 & 0 & m_b & 0 & 0 & 0 \\ 0 & 0 & 0 & 0 & m_{uf} & 0 & 0 \\ 0 & 0 & 0 & 0 & 0 & m_{ur} & 0 \\ 0 & 0 & 0 & 0 & 0 & 0 & J \end{bmatrix}$$

$$[C] = \begin{bmatrix} c_3 & 0 & -c_{se} & 0 & 0 & 0 & 0 \\ 0 & c_2 & -c_{se} & 0 & 0 & 0 & 0 \\ -c_3 & -c_2 & c_{se}+c_2+c_3 & -c_{se} & 0 & 0 & c_{se}a_3 \\ 0 & 0 & C_{se} & c_{(sh)f}+c_{(sh)r}+c_{se} & -c_{(sh)f} & -c_{(sh)r} & c_{sr}a_2-c_{(sh)f}a_1-c_{se}a_3 \\ 0 & 0 & 0 & c_{(sh)f} & 0 & 0 & c_{(sh)f} \\ 0 & 0 & 0 & -c_{(sh)r} & 0 & 0 & -c_{(sh)r}a_2 \\ 0 & 0 & c_{se}a_3 & c_{(sh)f}a_1-c_{(sh)r}a_2+c_{se}a_3 & 0 & 0 & -\left(c_{(sh)r}a_2{}^2+c_{(sh)f}a_1{}^2+c_{se}a_3{}^2\right) \end{bmatrix}$$

$$[K] = \begin{bmatrix} k_3 & 0 & -k_3 & 0 & 0 & 0 & 0 \\ 0 & k_2 & -k_2 & 0 & 0 & 0 & 0 \\ -k_3 & -k_2 & k_{se}+k_2+k_3 & k_{se} & 0 & 0 & k_{se}a_3 \\ 0 & 0 & -k_{se} & k_{sf}+k_{sr}+k_{se} & -k_{sf} & -k_{ur} & k_{sr}a_2-k_{sf}a_1-k_{se}a_3 \\ 0 & 0 & 0 & -k_{sf} & k_{uf}+k_{sf} & 0 & k_{sf}a_1 \\ 0 & 0 & 0 & -k_{sr} & 0 & k_{sr}+k_{ur} & k_{sr}a_2 \\ 0 & 0 & k_{se}a_3 & k_{sr}a_2-k_{sf}a_1+k_{se}a_3 & k_{sf}a_1 & -k_{sr}a_2 & k_{sf}a_1{}^2+k_{sr}a_2{}^2+k_{se}a_3{}^2 \end{bmatrix}$$

$$\{x\} = \begin{Bmatrix} x_3 \\ x_2 \\ x_{se} \\ x_b \\ x_{uf} \\ x_{ur} \\ \theta \end{Bmatrix} \quad \{\dot{x}\} = \begin{Bmatrix} \dot{x}_3 \\ \dot{x}_2 \\ \dot{x}_{se} \\ \dot{x}_b \\ \dot{x}_{uf} \\ \dot{x}_{ur} \\ \dot{\theta} \end{Bmatrix} \quad \{\ddot{x}\} = \begin{Bmatrix} \ddot{x}_3 \\ \ddot{x}_2 \\ \ddot{x}_{se} \\ \ddot{x}_b \\ \ddot{x}_{uf} \\ \ddot{x}_{ur} \\ \ddot{\theta} \end{Bmatrix}$$

$$[F_u] = \begin{Bmatrix} 0 \\ 0 \\ 0 \\ u_f + u_r \\ -u_f \\ -u_r \\ a_1 u_f - a_2 u_r \end{Bmatrix} \quad \text{and} \quad [F_z] = \begin{Bmatrix} 0 \\ 0 \\ 0 \\ 0 \\ k_{uf}z_f + c_{uf}\dot{z}_f \\ k_{ur}z_r + c_{ur}\dot{z}_r \\ 0 \end{Bmatrix} = \begin{Bmatrix} 0 \\ 0 \\ 0 \\ 0 \\ (k_{uf} + j\omega c_{uf})z_f \\ (k_{ur} + j\omega c_{ur})z_r \\ 0 \end{Bmatrix}$$

$\dot{z}_f = j\omega z_f, \quad \dot{z}_r = j\omega z_r$ are time derivative of z_f *and* z_r respectively

The vectors $\{z\}$ and $\{\dot{z}\}$ are displacement and velocity road inputs forcing functions

$[M]$, $[C]$ and $[K]$ are mass, damping and stiffness matrices;

$\{X\}$, $\{\dot{x}\}$ and $\{\ddot{x}\}$ are the acceleration, velocity and displacement vectors;

$[F_u]$ and $[F_z]$ are the force functions

2.2 Steady State Road Conditions

A steady state ride happens when a vehicle travels at a constant speed on a straight road. This is described by the power spectral densities (PSD) and it is expressed in **Eq. (34)** as:

$$PSD = \frac{C_r}{v^\alpha} m^3/cycle \tag{34}$$

Where

C_r = road roughness index
α = wavenumber (frequency characteristics of the road)

Converting the power spectral density to the function of road speed and frequency domain, PSD function is expressed in **Eq. (35)** as

$$PSD = \left(\frac{U}{f}\right)^\alpha \frac{1}{U} = C_r \frac{U^{\alpha-1}}{f^\alpha} \tag{35}$$

Where

U = vehicle speed (km/h), f is the frequency (Hz)

2.3 Semi-active Half-car Suspension System and Human Biomechanical Parameters

Appropriate parameters were selected for the vehicle suspension system characterization for ride analysis that entails how to minimize discomforts experienced by riders on the vehicle and the road holding analysis. The objective of the design is to reduce both the acceleration of the vehicle body and the suspension travel within the constraints of suspension space for a specific suspension system parameter set.

A mid-sized saloon car parameters were used. This is due to common use of this type of vehicles, their lower cost of purchase, effects of vibration on the vehicle riders and the rides' experience of the vehicles as they travel on different road conditions.

Table 1. The table shows suspension parameters [22]

Parameter	Symbol	Values	Unit
vehicle chassis Sprung mass	m_b	575	Kg
Vehicle's Moment of inertia	J	769	Kgm^2
Front axle Unsprung mass	m_{uf}	60	Kg
rear axle Unsprung mass	m_{ur}	60	Kg
front tire Stiffness	k_{uf}	190	kN/m
rear tire Stiffness	k_{ur}	190	kN/m
front tire Damping coefficient	c_{uf}	350	Ns/m
Rear tire Damping coefficient	c_{ur}	350	Ns/m
front axle Stiffness	k_{sf}	16812	N/m
rear axle Stiffness	k_{sr}	16812	N/m
Front axle Damping coefficient	c_{sf}	1000	Ns/m
Rear axle Damping coefficient	c_{sr}	1000	Ns/m
Front body length from C.G	a_1	1.4	M
Rear body length from C.G	a_2	1.4	M
Distance of seat from C.G	a_3	0.7	M

Table 2*. Biomechanical parameters of the human system [23]*

Parameter	Symbol	Values	Unit
Lower limb mass	m_2	5.5	Kg
Upper limb mass	m_3	36	Kg
Lower limb stiffness	k_2	144000	N/m
Upper limb stiffness	k_3	20000	N/m
Lower limb damping coefficient	c_2	909	Ns/m
Upper limb damping coefficient	c_3	330	Ns/m

2.4 Road Roughness Profile Parameters for Steady State Road Conditions.

The road roughness characteristics for different roads is shown in Table 3.

Table 3. *Road roughness characteristics*

Nature of road	Characteristics	Wavenumber	Roughness Index
Highway	Smooth road	2.1	4.8×10^{-7}
Pavement	Gravel road	2.1	4.4×10^{-6}
Suburban	Rough road	2.1	8.1×10^{-6}

2.5 Responses of Vehicle Suspension System to Steady Sate Road Condition

In order to investigate the dynamic response of vehicle traveling on different road surface roughness profiles, Simulink Block Diagram based on the dynamic equations of the model for steady state road roughness conditions was developed and shown in Figure 2.

Figure. 2. Simulink block diagram for steady state road surfaces.

3. Results and Discussions

3.1 Characteristics of Ride Performance of Vehicle Suspension System

Three parameters, that is, vehicle discomfort parameter, suspension working space, and dynamic tire load or force were used to assess the characteristics of ride conditions of vehicle suspension system traveling on steady state road conditions. The weighted rms of the acceleration of the vehicle body gives the discomfort parameter [24 – 26].

3.2 Discomfort Parameter of the Vehicle

When the human body is exposed to excessive vibration, the comfort, and in some cases, health and safety are impaired. Also, working efficiency of the human body is reduced. Increase in human exposure to vibration may lead to feeling of tiredness and reduction in tolerance to human vibration. The human body is most sensitive to vertical axis vibration in the region of 1Hz to 25Hz but the frequency of 4Hz to 8Hz are most critical. The weighted rms acceleration transmitted to the body in this frequency range is defined as the discomfort parameter. It is usually measured in terms of the vertical rigid body acceleration of the vehicle body.

There is need to evaluate the acceleration response of the vehicle body in the vertical direction over the frequency range in order to evaluate the passenger discomfort. This is achieved by applying appropriate parameters (human body sensitivity to vibration) which are then used for the response function. The parameter for discomfort is given by:

$$D = \int_{1}^{25} [[a(f)Q(f)]^2 df]^{0.5} \tag{36}$$

Where $a(f)$ = acceleration response function,

$Q(f)$ = weighting function for human body sensitivity to vibration.

The comfort of the rider is based on the vehicle's suspension system performance improved upon by implementing Skyhook and MR damper control strategy. Based on the vertical body acceleration of the rider in relation to comfort, suspension travel, and dynamic tire force at various vehicle speeds between 20km/h and 80km/h, the performance characteristics of the entire assembly of the suspension system of the vehicle are evaluated. The rider's body vibration exposure measurements for each day are evaluated and compared with values in Table 4 [27]. After implementing the skyhook control strategy, it is observed that the vertical body vibrations are within the human comfort zone. This is an improvement over what was observed in [6 – 7].

Table 4 shows the human comfort or discomfort range according to ISO 2631 [27] (Human comfort zone)

Table 4. Human comfort zone [27]

Vibration	Reaction
Less than 0.315m/s^2	Comfortable
0.315 to 0.630m/s^2	A little uncomfortable
0.5 to 1m/s^2	Fairly uncomfortable
0.8 to 1.6m/s^2	Uncomfortable
1.25 to 2.5m/s^2	Very uncomfortable
Greater than 2.5m/s^2	Extremely uncomfortable

3.3 Results

Figures 3 and 4 are the graphs of vertical body accelerations against speed of the vehicle when traveling on smooth, gravel, and suburban roads.
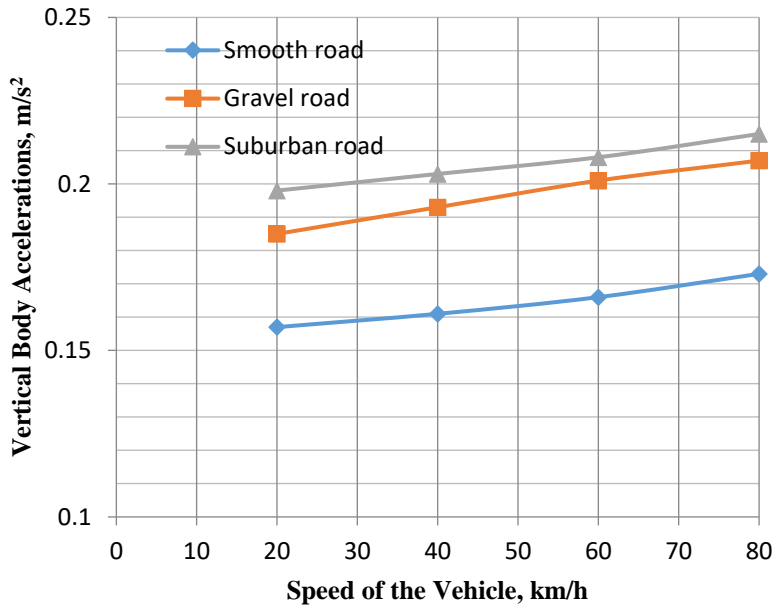
Figure. 3. Lower body vertical accelerations against Speeds of the Vehicle.
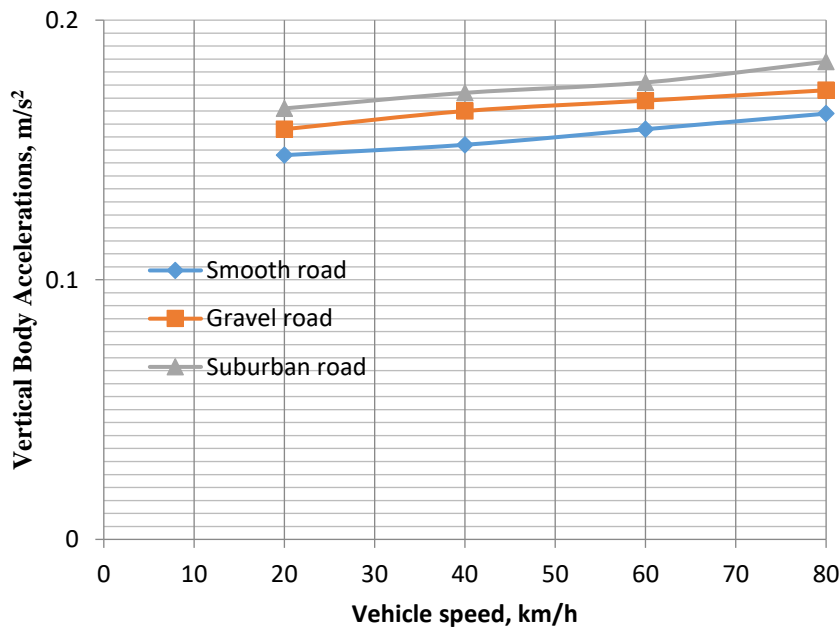
Figure. 4. Upper body vertical accelerations against speed of the vehicle.

Figures 5, 6 and 7 is the graph of vertical body accelerations and suspension stiffness. The graphs show that the vehicle occupants will have a good ride irrespective of the road conditions the vehicle is traveling on when the suspension stiffness is increased. This improvement is due to the use of skyhook and magneto-rheological damper on the vehicle.
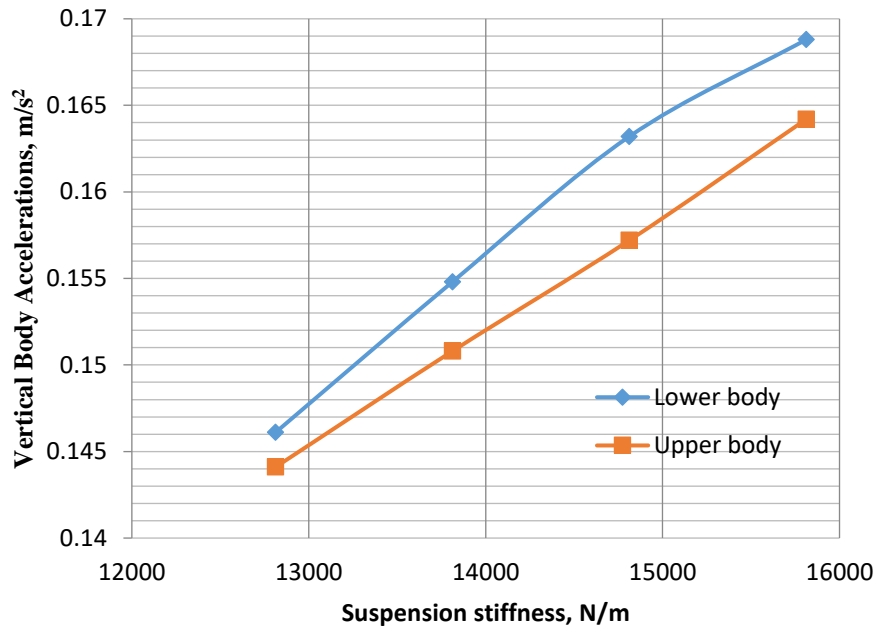
Figure. 5. Vertical Body accelerations against Suspension stiffness (Smooth Road).
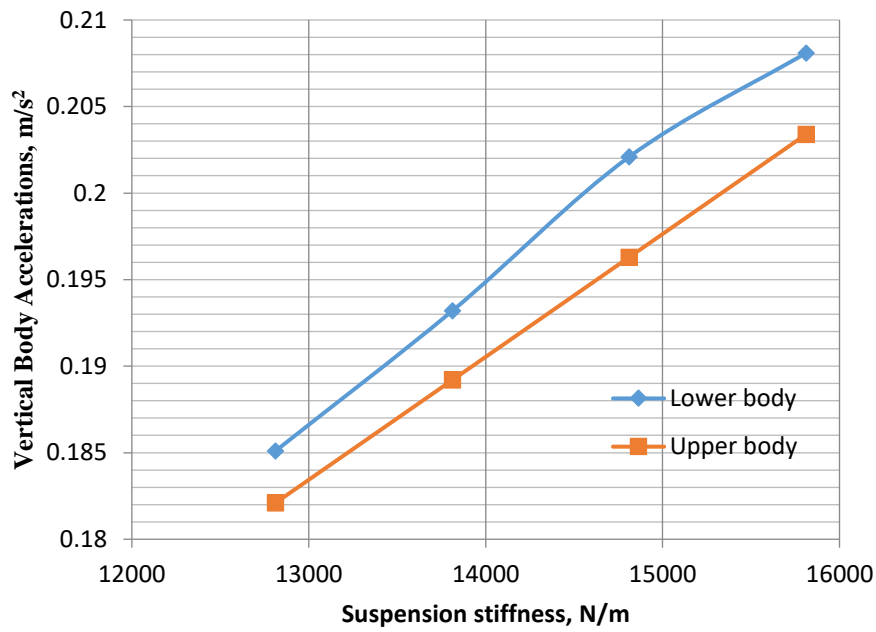
Figure. 6. Vertical Body accelerations against Suspension stiffness (Gravel Road).
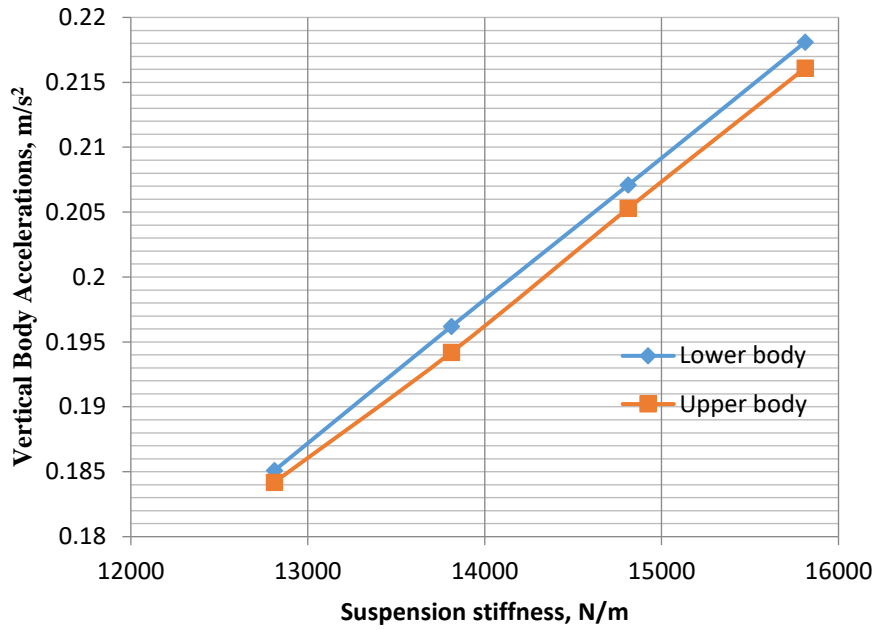
Figure. 7. Vertical Body accelerations against Suspension stiffness (Suburban Road).

Figures 8, 9 and 10 show the vertical body vibrations against tire stiffness as the vehicle travels on different road conditions. The result show that the human body experienced comfort irrespective of the roads when compared to ISO 2631 as the values are within the recommended human comfort level.
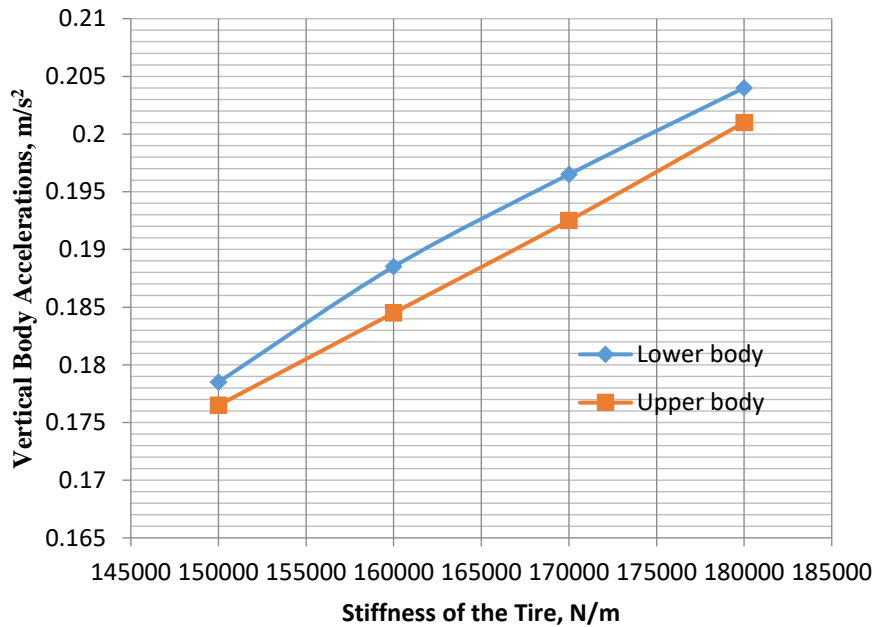
Figure. 8. Vertical Body accelerations against Tire stiffness (smooth road).
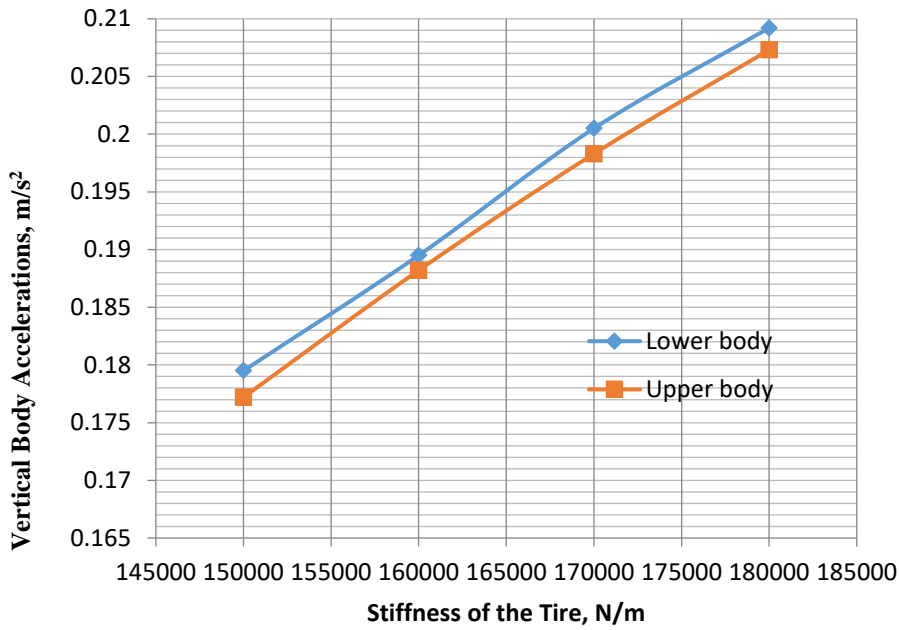
Figure. 9. Vertical Body accelerations against Tire stiffness (Gravel Road).
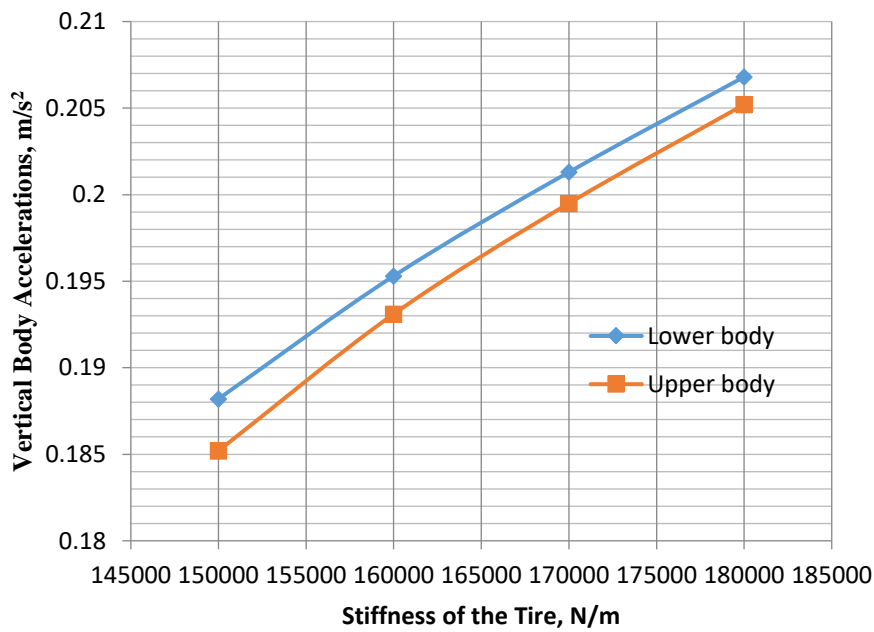
Figure. 10. Vertical Body accelerations against Tire stiffness (Suburban Road).

Figures 11, 12, and 13 is the graph of vertical body vibrations against the skyhook damping coefficient. show the effect of varying skyhook damping coefficient on human discomfort at the lower and upper parts of the body when vehicle traversed smooth, gravel and suburban road conditions.
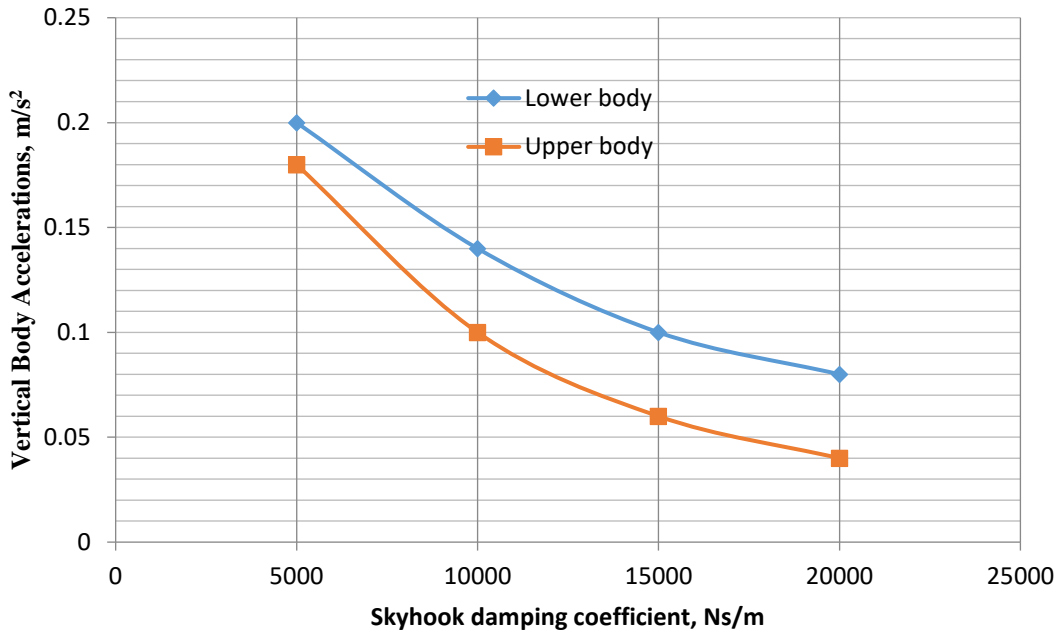
Figure. 11. Vertical Body accelerations against skyhook damping coefficient (smooth road)
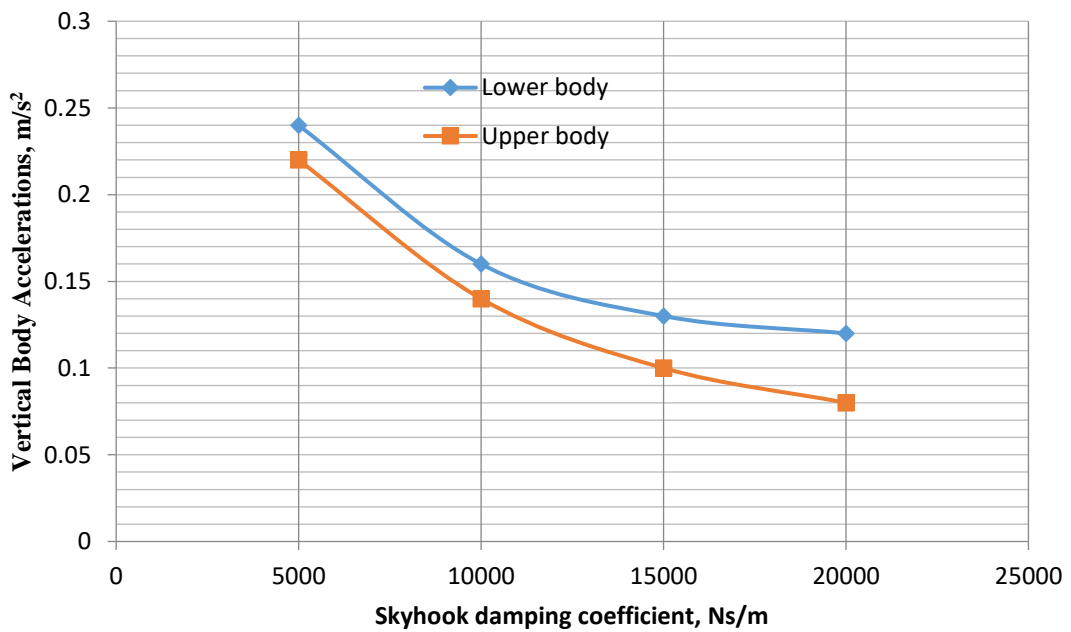
Figure. 12. Vertical Body accelerations against skyhook damping coefficient (gravel road)

Figure 13 also shows the effect of variation skyhook damping coefficient on human discomfort experienced at the lower and upper parts of the body when vehicle travels on suburban road. Increase in the skyhook damping coefficient decreases the discomfort experienced at the lower and upper parts of the body of the human body.
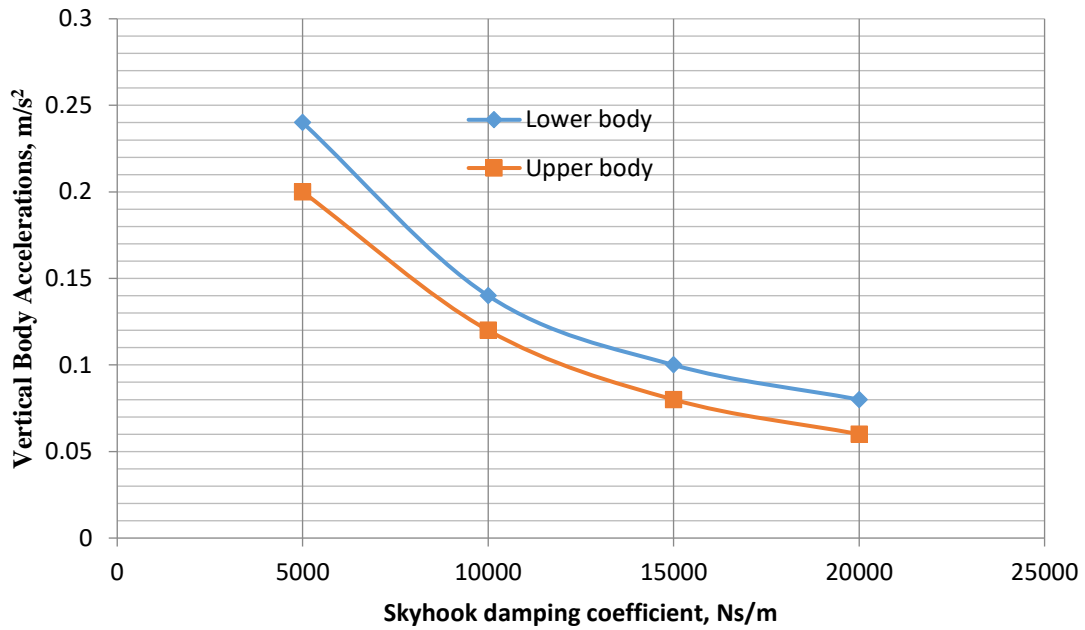
Figure. 13. Vertical Body accelerations against skyhook damping coefficient (suburban road)
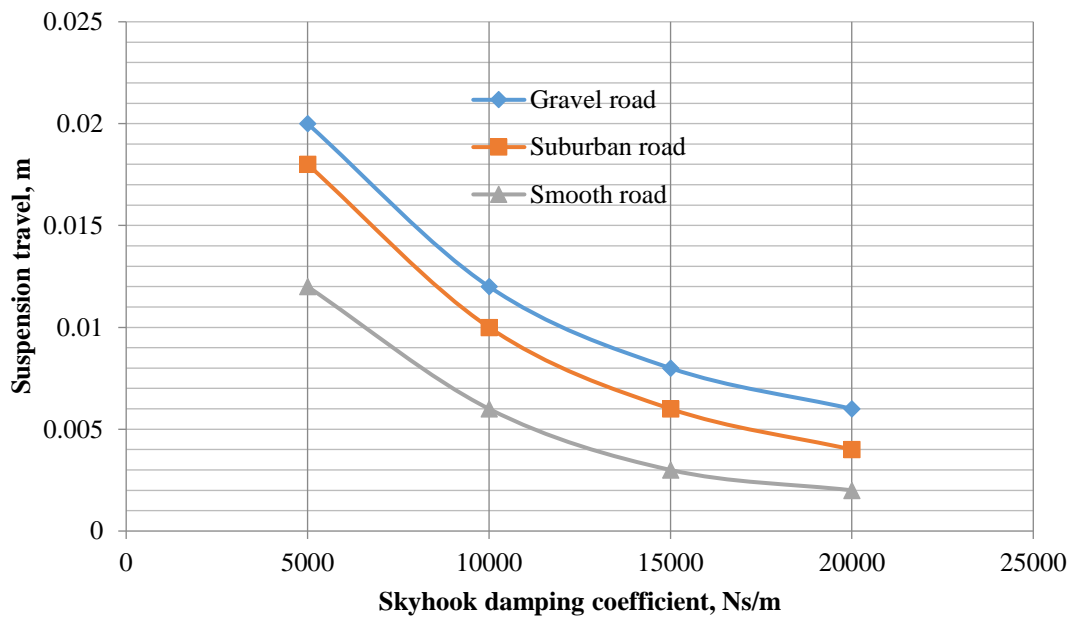
Figure. 14. Suspension travel against skyhook damping coefficient (steady state road conditions).

Figure 15 shows the effect of varying the skyhook damping coefficient on dynamic tire force of the vehicle. The result shows that the dynamic tire force gradually increased as the skyhook damping coefficient increased.
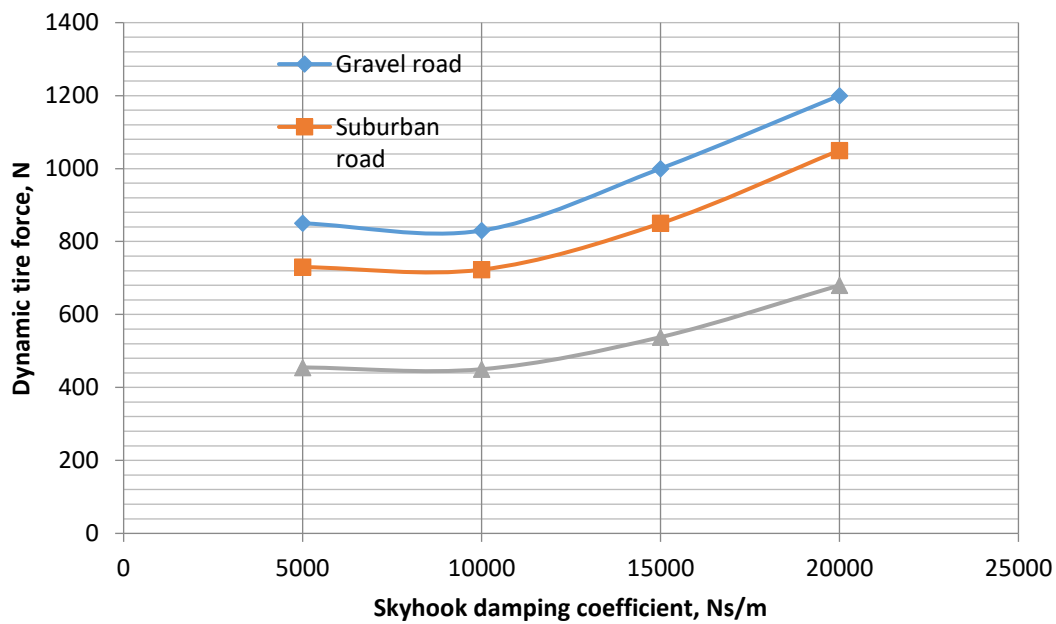
Figure. 15. Dynamic tire force against skyhook damping coefficient (steady state road conditions).

3.4 Discussions of Results

The researchers working in [6 – 7] used a half-car model with 7-degree of freedom. Therefore, the results obtained in this present work can be and will be compared with results obtained in [6-7] since the present work used half-model with 7 degree-of-freedom. This present work is actually a solution proffered to identify problems of excessive vertical body vibrations while passengers ride on vehicles. The maximum vertical body accelerations indicated against the maximum speed of 80 km/h of the vehicle when traveling on smooth, gravel, and suburban roads in Figure 3 and Figure 4 is 0.22 m/s^2. This value is less than 1.75 m/s^2 obtained in [6], less than 1.0 m/s^2 obtained in [7], and also less than 0.315 m/s^2, the maximum permissible daily dosage of vertical body acceleration as indicated in [27]. It is indicated in Figures 5 – 7 that the maximum vertical body acceleration is 0.218 m/s^2 which is less than 0.315 m/s^2 maximum permissible daily human dosage as the suspension stiffness of the vehicle is increases to 16, 000 N/m. This is less than 1.95 m/s^2 obtained in [6] and 0.5 m/s^2 obtained in [7]. In Figures 8 – 10, the maximum vertical body acceleration is 0.207 m/s^2, this is also less than the maximum threshold of 0.315 m/s^2 permissible by [27]. This is less than maximum values of 1.74 m/s^2 and 0.62 m/s^2 obtained in [6] and [7] respectively. The effect of increasing the skyhook damping coefficient of the vehicle suspension system as the vehicle travels on different road conditions are shown in Figures 11 – 13. These figures showed that the vertical body acceleration of the riders on vehicle decreased to a minimum from 0.2 - 0.04 m/s^2, 0.24 - 0.048 m/s^2 and 0.24 - 0.060 m/s^2 for the vehicle travel on smooth, gravel and suburban roads respectively as the skyhook damping coefficient is increased from 5, 000 to 20, 000 Ns/m. This leads to a great decrease in the discomfort experienced by the vehicle rider. This is definitely an improvement over what was observed in [6 – 7] where the vertical body accelerations increase and the damping coefficient increased from 0.245 – 0.260 m/s^2, 0 348 – 0.454 m/s^2, and 0.38 – 0.454 m/s^2 for the vehicle travel on smooth, gravel and suburban roads respectively. With this, it is clearly demonstrated that skyhook control strategy offered better comfortable ride to the riders traveling on smooth, gravel and suburban roads.

4. Conclusion

Skyhook control strategy has been applied to semi-active suspension system with magneto-rheological (M.R) damper to improve the performance of the suspension system of a vehicle traveling on a road with steady state conditions. The application of skyhook control strategy and magneto-rheological damper in vehicle suspension system gave superior suspension performance especially in comfort improvement, reduction in suspension travel compared with passive suspension system. With the application of skyhook and magneto-rheological damper, the vehicle occupant experienced vibration dose value (VDV) within the comfort zone range prescribed in [27], irrespective of the speed and road conditions. The results show that passenger vertical body accelerations reduced due to the reduction in the vertical acceleration of the vehicle body. The suspension travel is also reduced as the skyhook damping coefficient increased. Clearly, it is demonstrated that vehicle suspension with skyhook control strategy improves the performance of the vehicle ride experience in contrast to the same vehicle model without skyhook and MR damper as indicated in [6-7]. Developing countries with bad state of roads will benefit from this research in that their vehicles can be fixed with skyhook control strategy to improve the health of their road users.

Definition of Terms

Dampers	The mechanism that absorbs shock from the road profile thereby isolating the vehicle from prolong oscillations
Dynamic tire force	The force exerted on the ground by the tire
Half-car model	The right or left half car model with its rolls, pitch and bounce dynamics
Human biomechanical parameter	Modal parameters of human body (dimensions of human body for biomechanical analysis)
Magneto-rheological dampers	An actuator that stimulates the skyhook control without an external power source
Power spectra density	The distribution of energy across the frequency spectrum of vibration
Skyhook control strategy	A control strategy that reduces the resonance peak of vehicle body vibration traversing irregular road profiles in other to improve stability and ride quality
Sprung mass	The mass of the vehicle body and other accessories suspended above the suspension system
Suspension stiffness	The resistance force exerted by the suspension when it is compressed or stretched
Suspension travel	The displacement of a vehicle's wheel when it traverses irregular road profiles
Tire stiffness	The measure of the force or vertical tire load to deflection at specific points as the vehicle traverses the road
Unsprung mass	Mass of the suspension system of the vehicle and all other accessories attached to it such as brakes, wheels, linkages, tires, drive shafts etc
Vibration dose value	Measure of human body to effect of vibration

Nomenclature

a_1, a_2, a_3	Distances between the vehicle centre of gravity and the front and rear suspensions
c_2, c_3	Lower limb and upper limb dampers
C_{sf}, C_{sr}	Suspension damping coefficient of front and rear sprung mass
$c_{(sh)f}, c_{(sh)r}$	Damping coefficients of the front and rear suspension damper of skyhooks
C_{uf}, C_{ur}	Damping coefficients of front and rear suspension damper of unsprung mass
F_{df}, F_{dr}	The front and rear half-car suspension model damping forces
$F_{sf}, F_{sr}, F_{uf}, F_{ur}$	Vertical forces exerted on the system by the front suspension and rear suspension of sprung and unsprung masses
$F_{(sh)f}, F_{(sh)r}$	The forces generated by the skyhook damper at front and rear suspension
F_u, F_z	Force functions of front and rear control and road input
h_0	Road bump height
G	Vehicle center of gravity
J	Polar Moment of inertia of the vehicle
k_2, k_3	The lower and upper limb spring constants
K_c	Coupling coefficient

k_{se}, c_{se}	Spring and damper of seat
K_{sf} K_{sr}	Front and rear suspension stiffness of sprung mass
K_{uf}, K_{ur}	Front and rear suspension stiffness of unsprung mass
m_b	Mass of the vehicle body
m_{se}, m_2, m_3	Seat, lower limb and upper limb masses respectively
M_{Sf}, M_{sr}	Front and rear suspensions sprung masses
M_{uf}, M_{ur}	Front and rear suspensions unsprung masses
P_f, P_r	Points of connections of the front and rear suspension to the vehicle body
q_b, $\dot{q}_b$	Displacement and velocity of seat in the vertical direction
u_f, u_r	The front and rear suspension control forces
v_0	Vehicle velocity
w_b	Road bump width
x_b	The sprung mass vertical displacement about the centre of gravity
x_{se}, x_2, x_3	Seat, lower and upper limb displacements
$\dot{x}_{se}, \dot{x}_2, \dot{x}_3$	Seat, lower and upper limb velocities
$\ddot{x}_{se}, \ddot{x}_2, \ddot{x}_3$	Seat, lower and upper limb accelerations
x_{sf}, x_{sr}	The front and rear sprung mass vertical displacement about the center of gravity
x_{uf} x_{ur},	The front and rear unsprung mass vertical displacement
$z_f(t), z_r(t)$	The front and rear wheels sinusoidal road induced disturbance
$z, \dot{z}$	Road input function displacement and velocity
z_f, z_r	Disturbances at the front and rear due to the vehicle's traversing uneven road
$\dot{z}_f, \dot{z}_r$	The front and rear velocities due to road input
ω	Road distribution natural frequency
$\theta, \dot{\theta}, \ddot{\theta}$	Vehicle body's angular displacement, angular velocity and angular acceleration

References

[1] Blundel, M.V., (1991). The modeling and simulation of vehicle handling Part 1: analysis method, IMechE part K, *Journal of Multibody System Dynamics*. 213, 103 – 118.

[2] Griffin, M.J., (1990). *Handbook of human vibration*, Elsevier Academic Press, London.

[3] Jones, A.J., & Saunder, D.J., (1972) Equal body contours for whole body vertical, pulse sinusoidal vibration, *Journal of Sound and Vibration*, 23, 1 – 14.

[4] Niekerk, J.L; Pielemeier, W.J; Greenberg, J.A., (2002) The use of seat effective amplitude transmissibility (SEAT) values to predict dynamic seat comfort, *Journal of Sound and Vibration*, 260, 867 – 888.

[5] Mansfield, N.J., (2005). *Human response to vibration*, CRC Press, London.

[6] Ajayi, A. B., Ojogho, E., Adewusi, S. A., Ojolo, S. J., Campos, J. C. C., & Siqueira, A. M. de O. (2023a). Parametric Study of Rider's Comfort in a Vehicle with Semi-active Suspension System under Transient Road Conditions. The Journal of Engineering and Exact Sciences. 9(5). 15287–01e.

[7] Ajayi, A. B., Ojolo, S. J., Ojogho, E., & Siqueira, A. M. de O. (2023b). Parametric study of rider's comfort in a vehicle with semi-active suspension system under Steady State Road Conditions. *The Journal of Engineering and Exact Sciences.* (Fed. Univ. of Viçosa, Brazil), *9*(**5**), 15377–01e.

[8] Karnopp, D., (1990) Design principles for vibration control system using semi-active dampers, ASME Journal of Dynamic System, Measurement, Control 112, pp448-455.

[9] Shen, X., & Peng, H., (2003), Analysis of active suspension system with hydraulic actuators, Proceeding, IAVSD Conference, Japan

[10] Guglielmino. E., & Edge, K.A., A control friction damper for vehicle application, Center Engineering Practice, 12 pp. 431-443, 2004

[11] Huang, S.T., Choi, & H.Y., (2006) Adaptive sliding controller with seat tuning fuzzy compensation for vertical suspension control, Mechatronics, 16 pp.607-622.

[12] Du, H & Zhang, N. H (2007) Infinity control of active vehicle suspension with actuator time delay, Journal of Sound and Vibration 301, pp.236-252

[13] Ma, X., Wong, P., Zhao, J., Ying, H., & Xu, X., (2008) Design and testing of a non-linear model predictive controller for ride height control of automotive semi-active vehicle suspension system, IEEE Access, Vol. 6, pp.63777-63793.

[14] Tang, X., Du, H., Sun, S., Ning, D., Xing, Z., &Li, W., (2017), Takayi- sugeno fuzzy control for semi-active vehicle suspension with magneto-rheological damper and experimental validation, IEEE/ASME Transactions on Mechatronics, Vol. 22, no1, pp.291 – 300.

[15] Chen, M.Z., Hu, Y., & Li, C., (2016) Application of semi-active inerter in semi-active suspension via force tracking, Journal of Vibration and Acoustics, 138 (4), 1 – 11.

[16] Masi, J., (2001), Effect of control techniques on performance of semi-active damper, Master's Thesis, Mechanical Engineering, Virginia Polytechnic Institute and State University, Blacksburg, Virginia.

[17] Rajmani, R., (2006), *Vehicle Dynamics and Control*, Springer,2006

[18] Goncalves, F. D., (2001), Dynamic Analysis of semi-active control technique for vehicle applications, Virginia Polytechnic Institute and State University, Blacksburg, Virginia, 2001

[19] Karnopp, D., Crosby, M.J., & Harwood, R.A. (1974), Vibration control using semi-active force generator, ASME Journal of Engineering for Industry, 96, 619 – 626.

[20] Wu, X., & Griffin, M.J., (1997) A semi-active control policy to reduce the occurrence and severity of end-stop impacts in a suspension seat with an electro-rheological fluid damper, Journal of Sound and Vibration, 203, 5, 781-793.

[21] Liu, Y., Waters, T.P., Brennan, M.J., (2005) A comparison of semi-active damping control strategies for vibration isolation of harmonic disturbances, Journal of Sound and Vibration, 280, 21 – 39.

[22] Raji, A. V., (2013), Frequency response of semi-independent automobile suspension system, International of Engineering Research and Technology, 2(10), 654 – 661.

[23] Abbas. W., Abouelatta, O.B., El-Azab. M., Elsaidy, M., & Megahed, A. A., (2010), Optimization of biodynamic seated human model using generic algorithm, SCRIP Journal of Engineering, Vol. 2, 710 – 719.

[24] Olatunbosun, O.A., & Dunn, J.W; (1991). A simulation model for passive suspension ride performance Optimization, Automotive Simulation' 91 (M. Heller) Springer Verlag ,131 – 142.

[25] Sharp, R.S & Hassan, S.A, (1986), Evaluation of passive automotive suspension systems with variable stiffness and damping parameters. Vehicle System Dynamics, 15(6), pp335-350, 1986

[26] Abdel Hady, M.B.A & Crolla, D.A., (1989) Theoretical analysis of a active suspension performance using a four wheel vehicle model. Proceedings Institute of Mechanical Engineers, Vol. 203, Part D, PP. 125-135.

[27] ISO2631-1, Mechanical vibration and shock evaluation of human exposure to whole body vibration-Part 1: General requirements, International Organization for Standardization, 1997.